JOURNAL OF MATERIALS SCIENCE 27 (1992) 1892–1900

Characterization by XPS and SEM of reactive chemical vapour deposited boron carbide on carbon fibre

C. VINCENT, H. VINCENT, H. MOURICHOUX, J. BOUIX
Laboratoire de Physicochimie Minérale, associé au CNRS no. 116, Université Claude Bernard, Lyon 1, 43 boulevard du 11 Novembre 1918, 69622 Villeurbanne, Cedex, France

A process and apparatus used in the large-scale deposition of boron-based films on carbon fibres is described. The deposition occurs when the heated moving fibres react with a BCl_3–H_2 mixture. Among other advantages, such a process provides for continuous processing at atmospheric pressure. The properties of the as-deposited fibres, ex-Pan based, are discussed in terms of their use in material composites under ambient atmosphere. X-ray photoelectron spectroscopy shows that the filament surface consists of a B_4C–BN mixture.

1. Introduction

Carbon fibres are being considered for aerospace and aeronautical applications due to their light weight and excellent mechanical properties. A major drawback in using such fibres in oxidizing environments is that carbon reacts with oxygen, forming gaseous carbon oxides. During recent years, boron compounds have been identified as valuable engineering materials for coating carbon fibre because of their relatively good oxidation, their high hardness and high strength at elevated temperatures [1]. These coatings rely on the development of oxide films which provide protection by inhibiting oxygen diffusion. Boron carbide has been used for coating carbon fibre and C/C composite materials [2–4]. This material is usually produced by chemical vapour deposition (CVD). However, CVD often results in large grains of different compositions [5–8] which can produce larger flaws which limit strength, and textured deposits which result in poor protection. Recently, our laboratory has developed a process called "reactive chemical vapour deposition" (RCVD). The RCVD process consists in a reaction between the carbon and a reactive gaseous mixture, to a formation of a carbide layer on the substrate surface and a carbon diffusion in the carbide layer. RCVD is a method making possible the continuous preparation of homogeneous carbide-layers on carbon fibres, so SiC and TiC layers have been produced on various carbon fibres [9–12].

The purpose of this work was to study this new process to obtain more resistant carbon fibre. This paper is concerned with detailed investigations of the B_4C deposition process, the characterization of the surface fibres and the influence of the boron content on the tensile strength of the carbon fibres and on the oxidation behaviour of these coated fibres.

2. Experimental procedure

The experimental system used for the treatment is schematically shown in Fig. 1. The deposition chamber was a tubular quartz chamber, 28 mm diameter. Hydrogen and trichloride boron were introduced through an injector into the cell. The fibre was heated by Joule effect. The temperature was monitored by a bichromatic pyrometer and a electric power regulator. Trichloride boron was selected as the source of boron. The selection of RCVD run time was made by monitoring fibre speed, and hydrogen and trichloride boron flows were monitored through the use of electronic mass flowmeters. The mixture is defined by the molar ratio, R, or the flow ratio, between hydrogen and boron trichloride.

Polyacrylonitrile (PAN)-based carbon fibre (Toray T300) was used in this study. The fibre is constituted of a bundle of 6000 single filaments, the diameter of each filament is around 7 μm.

The resultant deposits were characterized by optical and scanning electron microscopy (SEM) for surface topography, and by X-ray diffraction technique (XDR) and X-ray photoelectron spectroscopy (XPS) for phase and composition identification. Microprobe electronic analysis and chemical analysis were also

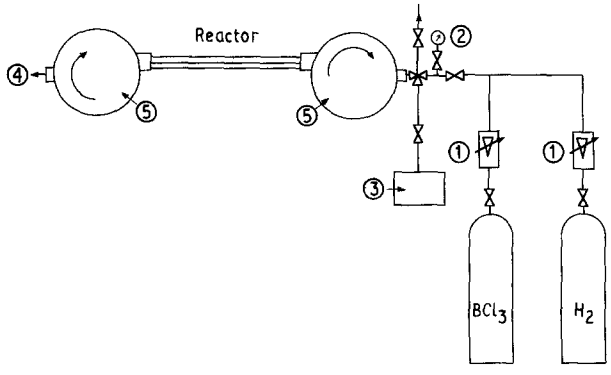

Figure 1 Schematic view of the RCVD equipment. 1, Flow meter; 2, pressure gauge; 3, vacuum pump; 4, gas outlet; 5, pulleys.

0022–2461

performed. Microstructural analyses were conducted on filament surfaces and polished sections and fractured surfaces. Tensile strength and modulus were evaluated using rupture tests on elementary filaments and the results were analysed by Weibull statistics. Rupture tests were conducted in air at room temperature on as-deposited and initial filaments, with a gauge length of 20 mm. The specific surface was determined by the BET method using nitrogen as adsorption gas.

Oxidation was carried out at 450, 600 and 700 °C in ambient air. For oxidation tests, 30 cm fibre lengths were suspended in the constant temperature zone of a furnace of a thermogravimetric device.

3. Results and discussion

3.1. Dependence of deposition rate on experimental conditions

The various RCVD conditions used in this work are summarized in Table I.

Chemical analysis showed that the deposition temperature, deposition run time and the mixture ratios are of some significance in deposition rate. Fig. 2a

TABLE I RCVD conditions and main mechanical properties of as-treated fibres

	T (°C)	R	dt (cm^3 min^{-1})	t_{ps} (min)	B (%)	C (%)	N (%)	O (%)	L_c (nm)	d_{tex} (g km^{-1})	σ_R (MPa)	E (GPa)	m
T300	–	–	–	–	–	93.1	7.3	0.05	1.52	382	3150	210	6.9
1	1330	0.5	15	2	0.8	96	2.7	0.1	2.4	376	3020	205	3.6
2	1330	1.5	25	2	2.1	95	3	0.2	2.6	379	2810	200	3.6
3	1330	10	110	1	1.6	95	2.9	0.1	2.1	390	2890	210	3.3
4	1330	10	110	2	3.2	93	3.4	0.1	2.1	383	2870	220	3.6
5	1330	10	110	2	3.2	91	3.6	0.1	2.1	388	–	–	–
6	1050	10	110	2	1.2	94	5.7	0.1	1.52	394	3120	215	4.5
7	1200	10	110	2	1	95	2.7	0.3	1.91	384	2860	225	4.4
8	1430	10	110	2	2.5	94	2.2	0.2	2.3	386	2530	240	4.2
9	1430	1.5	25	2	2.3	94	1.9	0.1	2.4	390	2240	230	3.5
10	1700	1.5	25	2	2	97	1.6	0.3	3.5	374	2620	225	4.7
11	1330	1.5	25	4	6	91.7	1.52	0.3		397	–	–	–
12	1330	1.5	25	15	6.2	90.4	2.7	0.3		395	–	–	–
13	1330	1.5	25	30	7.9	89.2	2.5	0.1		392	–	–	–
14	1330	1.5	75	1	3.5	92.6	3.4	0.1	2.1	391	3010	210	4.0
15	1330	1.5	75	2	4.1	92.5	3.4	0.2	2.4	389	3060	195	4.5
16	1330	1.5	75	3	–	–	–	–	2.4	396	–	–	–

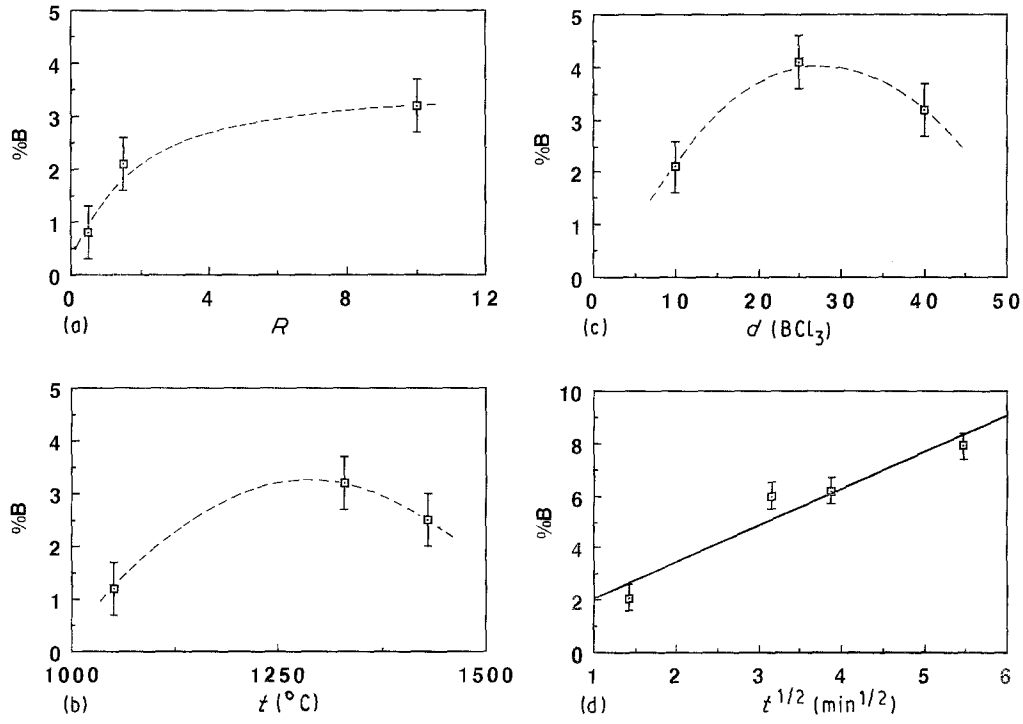

Figure 2 Evolution of B% as a function of: (a) H_2/BCl_3 (R) ratio, conditions: run time 2 min; total flow 110 cm^3 min^{-1}; (b) RCVD temperature, conditions: run time 2 min, total flow 110 cm^3 min^{-1}; (c) BCl_3 flow, conditions: run time 2 min, H_2/BCl_3 ratio 1.5; (d) square root of run time, conditions: H_2/BCl_3 ratio 1.5, total flow 25 cm^3 min^{-1}.

shows the increase of boron percentage for different BCl_3/H_2 mixtures at 1350 °C and for the same total input flow: hydrogen partial pressure appeared to increase the percentage of boron carbide.

It is seen that at a temperature above 1000 °C, the boron percentage is temperature dependent (Fig. 2b). For a total flow equal to 110 $cm^3 min^{-1}$, the boron percentage is hardly temperature dependent, as one would expect for a growth rate determined by diffusion in a solid phase, but it goes through a maximum at around 1350 °C. This behaviour can be explained by the presence of a boundary layer and by the diffusion of reactive gases through this boundary layer in the cold-wall reactor, and by the porous nature of the substrate and through the filaments of the bundle. At high temperature, the infiltration of the bundle by the gas mixture is poor, and the inner filaments are not treated. However, if the total flow is reduced, the maximum boron percentage is shifted to a higher temperature. For a flow of 25 $cm^3 min^{-1}$, no maximum in the boron per cent versus temperature curve is found in the temperature range studied.

It is seen that initially the boron percentage increases linearly with increasing input flow of BCl_3 for the same H_2/BCl_3 ratio (Fig. 2c); for a flow above 50 $cm^3 min^{-1}$, it then goes through a maximum.

As shown in Fig. 2d, the boron percentage increases linearly with the square root of the treatment time at a given temperature (1330 °C), i.e. consistent with a diffusion-limited growth. From these results, the optimal RCVD conditions are found to be $T = 1330$ °C, total flow = 25 $cm^3 min^{-1}$, and H_2/BCl_3 ratio in the range 1.5–10.

3.2. Characterization by XDR and XPS spectroscopy

Fibre samples were selected at random from a spool of coated fibre. X-ray diffraction patterns were obtained with a Philips PW 1840 diffractometer using CuK_α radiation with a nickel filter as the characteristic X-rays. Fig. 3 shows X-ray diffraction patterns of T300 fibre treated in a BCl_3/H_2 gas atmosphere at 1330 °C for various durations from 2–15 min. Very broad diffraction lines are seen for the initial fibre. In the X-ray diffraction patterns of the fibre treated for 2 and 15 min, the Bragg angle of carbon was shifted to a higher angle and the diffraction lines corresponding to B_4C appear but their intensities are very small. The apparent crystalline size, L_c, of the carbon was calculated from the half-width, β, of the (0 0 2) line using Scherrer's formula

$$L_c = 0.9\lambda/\beta\cos\theta \quad (1)$$

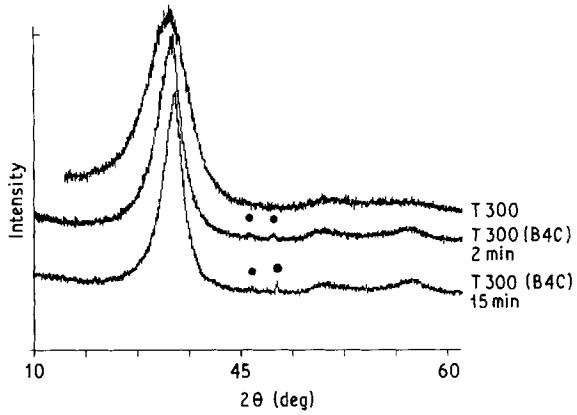

Figure 3 X-ray diffraction patterns of T300 fibre and T300 (B_4C) fibre treated for 2 and 15 min.

where λ is the wavelength of the X-rays, and θ is the diffraction angle. The size, L_c, increased with the RCVD treatment temperature.

The fibres were also analysed by XPS, using the monochromatic AlK_α radiation ($h\nu$ = 1486.6 eV) of a 5950 Hewlett-Packard photoelectron spectrometer with an overall resolution of 0.8 eV. The bundles of fibres were put on a copper foil. The pressure in the spectrometer was in the 10^{-8}–10^{-10} torr range. They were etched for 2 min by argon ion bombardment with an ion gun (2 keV incident energy). A XPS survey spectrum revealed carbon, boron, oxygen and nitrogen. Disymmetrics and linewidths of the main C_{1s} and B_{1s} show that these signals do not correspond to a unique chemical form. In order to resolve the different chemical components in the fibre, a computerized procedure was undertaken. Theoretical C_{1s} and B_{1s} spectra were constructed by addition of Gaussian–Lorentzian components, each component being representative of a chemical entity. Modification of the intensity of the component was allowed until the best fitting between experimental and calculated spectra was obtained.

The binding energies of different compounds, found in the literature, are reported in Fig. 4. Table II gives the binding energies and the normalized areas of the different components deduced from this resolution procedure. As shown in Fig. 5a and b the presence of four chemical components (labelled I, II, III, IV) for the C_{1s} photopeak and two components (labelled I, II) for the B_{1s} photopeak is evident, thus indicating the chemically complex nature of the fibre surface. The components C_I, C_{II} and C_{III} are characteristic of carbon fibre; they could be attributed to molecular groups C–O, C=O [13] and will not be discussed further. The component C_{IV} corresponds to carbon from a carbide such as B_4C.

TABLE II Binding energies and relative intensities of the different components deduced from computerized procedure

	C_{1s}				B_{1s}		N_{1s}
	C_I	C_{II}	C_{III}	C_{IV} (B_4C)	B_I (BN)	B_{II} (B_4C)	BN
E_I	284.3	286.0	288.5	281.8	189.8	186.6	397.5
Norm. area	35484	10219	1590	2368	13353	7219	23450

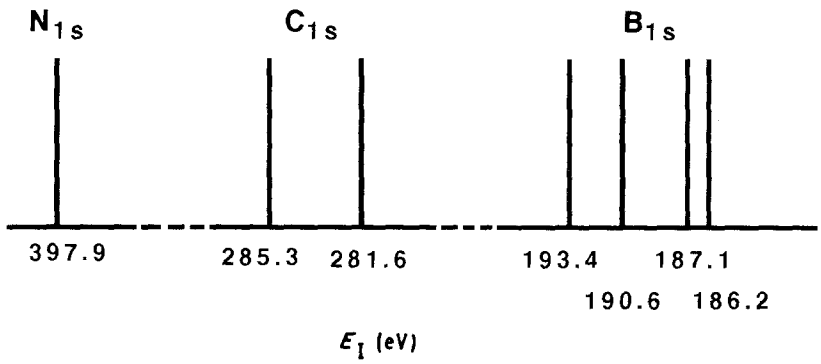

Figure 4 Binding energies of different compounds of carbon, boron and nitrogen.

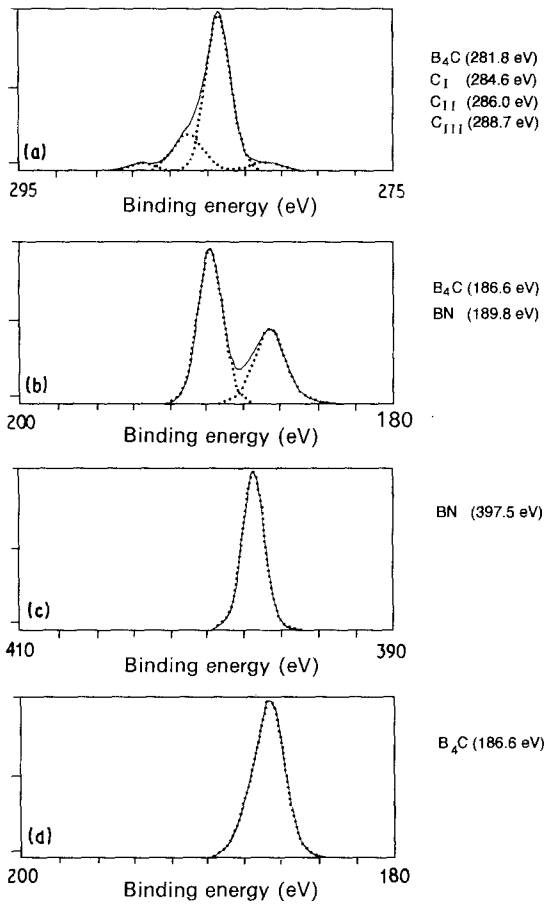

Figure 5 Analysis of photopeaks: (a) C_{1s}; (b) B_{1s}; (c) N_{1s}; (d) B_{1s} (pitch fibre RCVD coated by B_4C).

The attribution of components B_I and B_{II} in B_{1s} is also unambiguous (Fig. 5b). Component B_I corresponds to boron from boron carbide. After correcting the intensities of the C_{1s} and B_{1s} photopeaks for their respective photoionization cross-section, the composition of the carbide could be evaluated from the components C_{IV} and B_I. Such elementary composition is consistent with B_4C formula. The component B_{II} corresponds to boron from BN [15]. The N_{1s} signal (Fig. 5c) demonstrates that the component B_{II} in B_{1s} is correlated with the presence of boron nitride. This result is surprising, and shows the important role of the impurities in the fibre or in the reactor during the RCVD process. It is worth noting that this nitride is never formed during the B_4C RCVD on pitch fibres (Fig. 5d). An evident explanation comes from the composition of the fibres: the quantity of nitrogen found in Pan fibre and in pitch fibre vary to a very large extent. In the preparation process of the fibre from polyacrylonitrile, a significant nitrogen content is incorporated by incomplete conversion of the polymer chain to carbon, and during the RCVD process, one important part of the nitrogen atoms reacts with the BCl_3–H_2 mixture, and remains incorporated into the layer in the BN form. The nitrogen percentage found in such an as-treated fibre is higher than that found in a T300 fibre heated at the same temperature, but in an inert atmosphere.

The relative intensities of the B_I and B_{II} components in the B_{1s} peak evolve with boron content in the fibre: for less than 4% B, the B_I intensity is higher than the B_{II} intensity; on the contrary, for more than 4% B, the intensity of the component B_{II} from B_4C is higher than the intensity B_I from BN. It seems that BN formation is easier than B_4C formation.

In this paper, in spite of a BN presence in the layer, the fibre treated by RCVD in the BCl_3–H_2 gas phase will be called T300 (B_4C).

3.3. Room-temperature tensile behaviour

Table I gives the main mechanical properties of the as-treated and uncoated carbon fibres. In all cases, it was found that the coated fibres have a higher modulus compared to uncoated fibres. The increase in the modulus arises from the presence of a boron compound layer, for example the B_4C modulus is superior to T300 modulus, 490 and 210 MPa, respectively. The strength distribution for a fibre sample with constant gauge length presented as a plot of $\ln\ln(1/P_s)$ versus $\ln\sigma$, yields one or two straight lines with one or two slopes, m (Fig. 6). For a short run time (1–2 min), at 1050 °C, the RCVD treatment was found to improve the tensile strength (3500 MPa instead of 3100 MPa) and at 1700 °C, this treatment leads to two kinds of filament with different mechanical properties. The Weibull plots show two straight lines. The portion of the curve with a much lower slope occurring in the lower strength range can possibly be attributed to a sparse population of large defects, as large crystals and bridges between single filaments and small pits on the surface as shown in the scanning electron micrographs. In the 1200–1500 °C range, the results of the tensile strength tests indicate an average strength, σ_R, around 2500–3000 MPa, a slightly lower value than

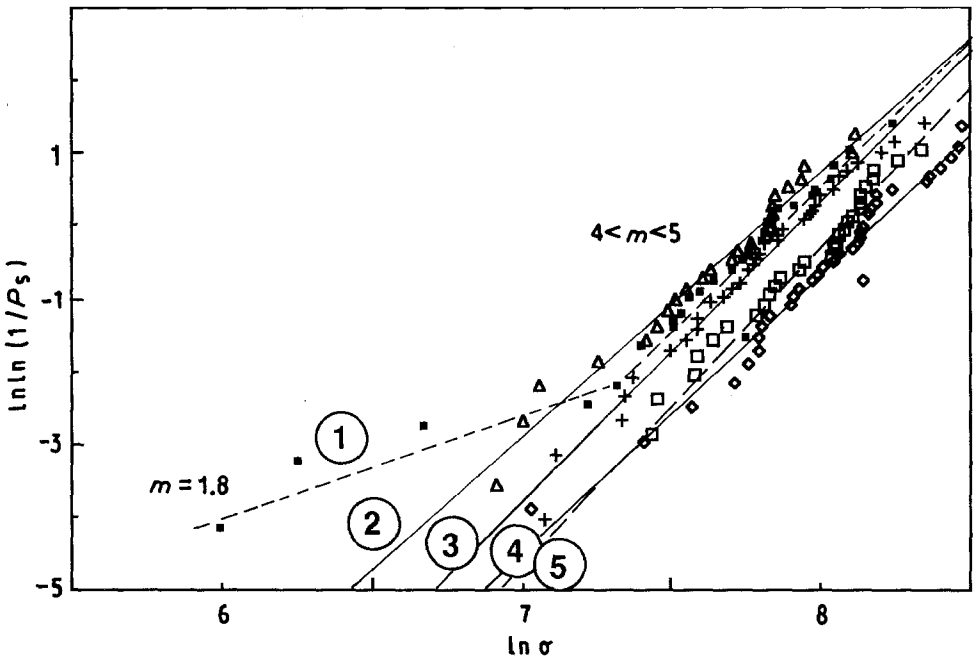

Figure 6 Evolution of Weibull plots for filaments as a function of RCVD parameters. 1, 1700 °C 2 min, 1.8% B. 2, 1350 °C, 2 min, 2.1%B. 3, 1350 °C 2 min, 2.8% B. 4, 1050 °C, 2 min, 1.3% B. 5, 1350 °C, 22 min, 6.2% B.

that of the initial fibre. The value of the tensile strength seems to be independent of the boron percentage. The same Weibull parameter, m, of around 4, is found; thus, this result suggests that the defects do not develop differently according the chemical composition and the same kind of defects, i.e. mainly surface defects, are controlling the failure of the treated RCVD filaments.

For longer RCVD times, the degradation of the mechanical properties becomes critical over 4 min.

3.4. Oxidation behaviour

The kinetics of oxidation of boron compounds is dependent on the atmospheric composition: the rate is much slower in dry air than in wet air. In this work, the oxidation tests are performed in an ambient atmosphere to verify the protective effect of the coating on the behaviour of fibres under normal use conditions. Thermogravimetry (TG) curves of T300 (B_4C) fibres were obtained to examine the profile of the oxidation process with a Setaram TG apparatus in an ambient atmosphere. 70 mg fibre were suspended with a platinum wire in the furnace. The samples were treated up to 1100°C in air at a heating rate of 250 °C h^{-1}, or at a given temperature. Isothermal runs were made at temperatures between 450 and 700 °C.

Typical weight loss data for T300 (B_4C) fibres as a function of temperature are shown in Fig. 7. The weight losses are always smaller for the as-deposited fibres than the uninhibited fibre. The oxidation process can be discussed in three stages: up to T_1, T_1–T_2 and above T_2. The respective temperatures from T_1 and T_2 were determined by the point of deflection in the TG curve. One stage is observed in the TG curve of T300 fibre.

In the 20 °C–T_1 temperature range, weight loss is nil, and the coating protects the fibre. The change due

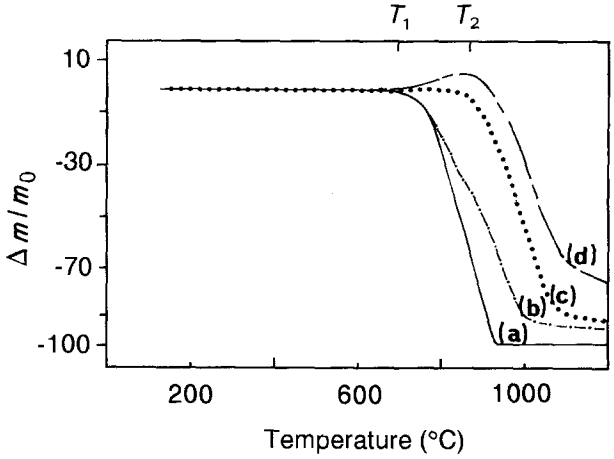

Figure 7 TG curves of T300(B_4C) versus boron content. Conditions: ambient atmosphere, heating rate 250 °C h^{-1}. (a) T300, (b) 1.1% B, (c) 2.3% B and (d) 3.3% B.

to the heat treatment in the T_1–T_2 range is mainly a weight increase caused by reaction between B_4C and oxygen

$$B_4C + 3\,O_2 \rightarrow 2\,B_2O_3 \qquad (2)$$

In the third stage above T_2, the weight loss is as large as in the single stage of the unprotected fibre. After combustion of carbon, the residual weight is dependent on the boron content of the tested fibre.

At constant temperature, between 450 and 600 °C, the weight losses remains negligible for several hours and the boron layer seems to be a good diffusion barrier layer. For example, at 600 °C, Fig. 8 shows the TG curves for various coated fibres. All the curves show the same two regions followed by a third region of decreasing slope. The apparent reaction rate in this region can be measured from the linear portion of the weight loss–time curve. It is evident that the oxidation rate decreases when the boron content increases; after 4 h, for 0.4% B, the weight loss is 50%, for 3.3%

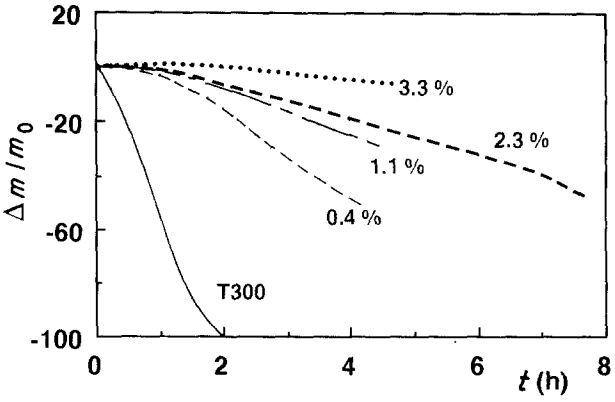

B, it is around 0. The interpretation of the weight change data is complicated by the fact that the decrease may partially result from the weight gain associated with formation of boron oxides, and by possible evaporation of volatile boron–oxygen species. The oxidation rate increases with air temperature; at 700 °C, the combustion is total after 4 h, the thickness

Figure 8 TG curves of T300(B_4C). Conditions: ambient atmosphere, isothermal heating (600 °C).

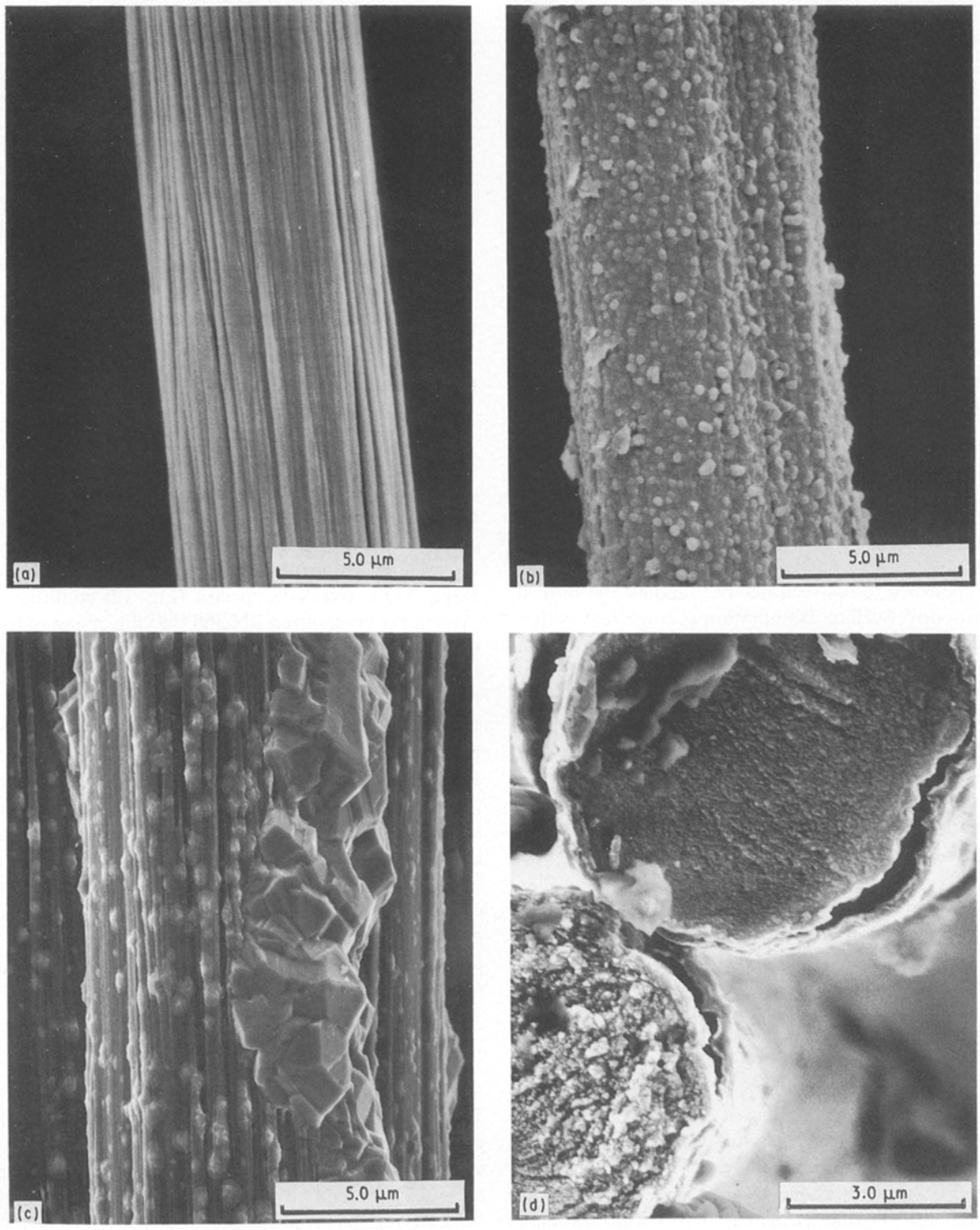

Figure 9 Evolution of surface morphology by SEM examination as a function of RCVD temperature (2 min run time). (a) 1350 °C, (b) 1400 °C, (c) 1500 °C, (d) 1500 °C (cross-section).

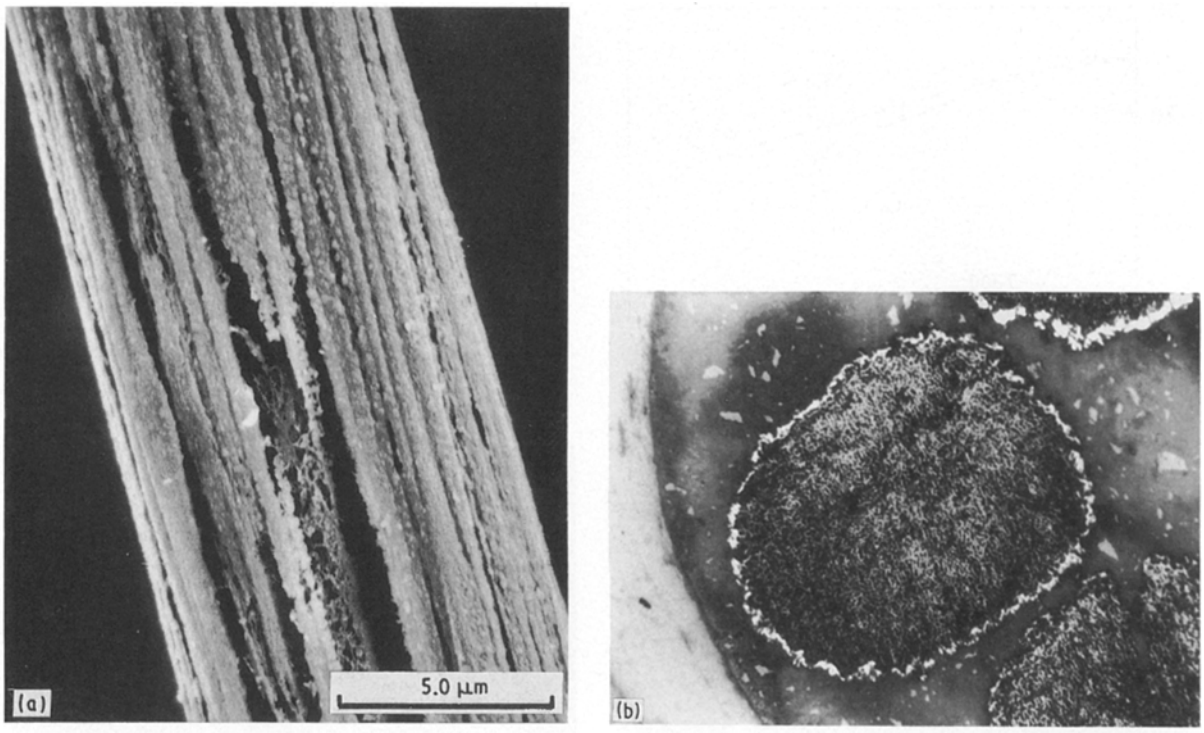

Figure 10 Morphology of T300 (B_4C) after an RCVD run time of up to 6 min at 1330 °C. (a) Scanning electron micrograph of a single filament; (b) optical micrograph of a bundle section.

of the boron layer is not sufficient to inhibit oxidation for a long time.

3.5. Characterization by SEM

As an aid to interpreting tensile strength and oxidation test results, filaments were examined by SEM and polished cross-sections of bundles by optical microscopy. Surface examination is consistent with a lowering of the strength. Fig. 9a–c show differences in the as-deposited surface and the grain structure obtained by changing the RCVD parameters. Note the texture surface for high-temperature treatment and long duration in contrast to the smooth surface topology and its extremely fine grain if the RCVD conditions are those mentioned above. For example, at temperatures above 1400 °C, boron carbide was enhanced and tended to cause a nodular deposit. At 1500 °C, large crystals can be formed on some filaments. In this case, the irregular coating remains continuous but variable in thickness; it is not always tightly bonded to the filament (Fig. 9d), this phenomenon arises because the thermal expansion coefficient mismatch between the fibre and a thick coating causes the coating to crack. Contrary to this observation, no spalling at the layer could be detected in the RCVD temperature range 1100–1400 °C. It should be noted that the specific surface increases rapidly when the RCVD temperature duration increases. Up to 1400 °C, the specific surface of the T300 (B_4C) fibre is around 0.5 $m^2 g^{-1}$; above 1500 °C, it is 1 $m^2 g^{-1}$.

If the RCVD time is increased to 6 min, the filaments have pits on the surface (Fig. 10a). The deposit thickness is large at the periphery of the bundle, and the external filaments can be bonded by bridges (Fig. 10b).

Fig. 11a–c show scanning electron micrographs of T300 (B_4C) fibres after air treatment at 600 °C. The change is a function of oxidation run time. Just after the total burn off of the carbon core, the residue consists of a thin and continuous shell that replicates the crenulated morphology of the T300 fibre. At this stage, XDR and XPS spectra (Fig. 12) confirm the presence of crystallized BN and the conversion of B_4C to B_2O_3 glass. On increasing the oxidation run time, the surface morphology changes. Initially the shell becomes discontinuous, and then the shell disappears. Under these oxidizing conditions, the boron compounds are converted to boron oxide glasses which are sufficiently fluid to form non-wetting beads on the filament surface: the quality of the shell becomes insufficient to protect the fibre from oxidation, and carbon burns under the shell (Fig. 11c). The transition from a continuous shell to a discontinuous shell can explain why the RCVD layer protection evolves with oxidation time. The phenomenon is amplified by the fact that the oxide reacts with wet air to form volatile species.

4. Conclusion

The XPS analysis of carbon fibre treated in a BCl_3–H_2 mixture performed on a bundle of fibres reveals a surface modification, with the layer formed containing carbon, boron and nitrogen atoms. The chemical entities entering the layer are B_4C and BN. Up to 600 °C, in air atmosphere, the weight loss of the as-protected fibre is negligible, boron compounds are oxidized in

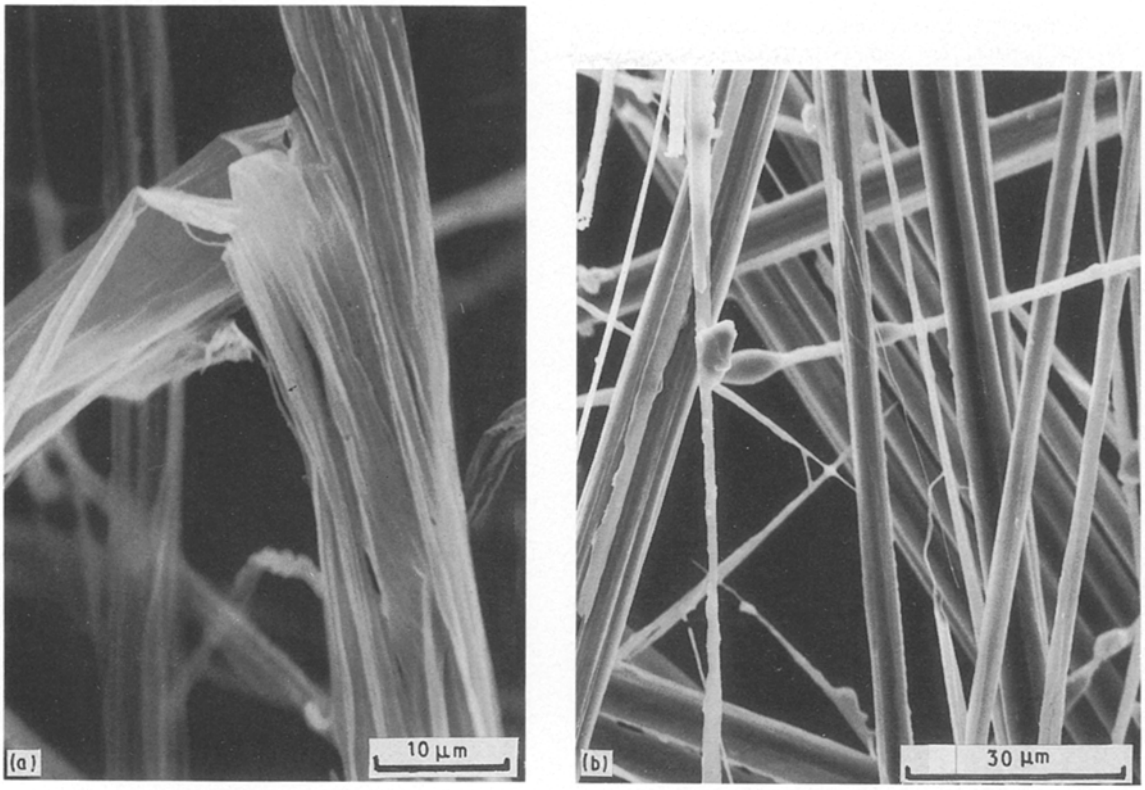

Figure 11 Evolution of surface morphology by SEM examination as a function of oxidation time. (a) after 24 h oxidation at 600 °C; (b) presence of non-wetting beads of B_2O_3 glass; (c) carbon burning under the shell.

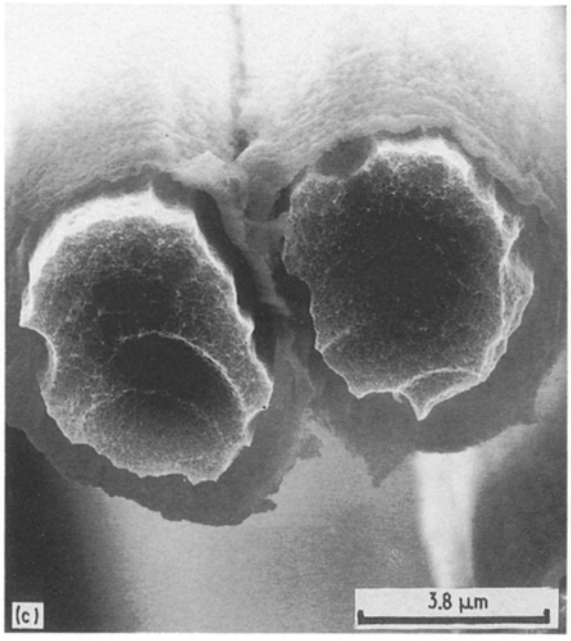

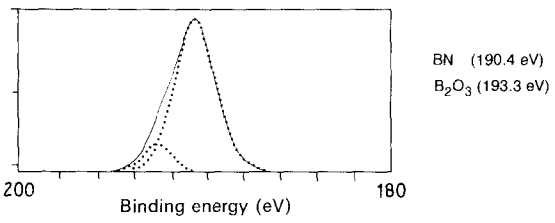

Figure 12 Photopeak B_{1s} after oxidation at 600 °C. Only the peak from BN remains.

boron oxide and the new layer is a excellent diffusion barrier. The shell morphology evolves with oxidation time; the continuous shell becomes discontinuous, and its change explains why the protection is limited after several hours.

Acknowledgement

This work was performed under contract to the Direction de la Recherche et des Etudes Techniques (DRET). The authors are grateful for its financial aid.

References

1. D. W. MCKEE, "Chemistry and Physics of Carbons", Vol. 16, edited by P. L. Walker Jr and P. A. Thrower, (Marcel Dekker, New York, 1981) p. 1.
2. J. B. HIGGINS, A. GATTI and J. H. GEGHARDT, *J. Electrochem. Soc.* **116** (1969) 137.
3. D. MORIN, *J. Less-Common Metals* **47** (1976) 207.
4. R. PAILLER, Doctorat ès-Sciences, Bordeaux, France (1979).
5. I. M. MACKINNON and B. G. REUBEN, *J. Electrochem. Soc.* **122** (1975) 806.
6. K. PLOOG, *J. Crystal Growth* **24/25** (1974) 197.
7. D. N. KEVILL, T. J. RISSMZAN, D. BREWE and C. WOOD, *J. Less-Common Metals* **117** (1986) 421.
8. U. JANNSON and J. O. CARLSSON, *Thin Solid Films* **124** (1985) 101.
9. J. C. VIALA, J. BOUIX, H. VINCENT, J. L. PONTHENIER, J. DAZORD and C. VINCENT, Fr. Pat. 86 17157, 4 December (1986).
10. J. BOUIX, C. VINCENT, J. L. PONTHENIER, J. DAZORD and H. VINCENT, US Pat. 4 859 503, 22 August (1989).
11. H. VINCENT, C. VINCENT, J. L. PONTHENIER, H. MOURICHOUX and J. BOUIX, in "Development in the Science and Technology of Composite Materials", edited by

A. R. Bunsell, P. Lamicq and A. Massiah (Elsevier Applied Science, London, New York, 1989) p. 257.
12. H. MOURICHOUX, J. BOUIX, B. BONNETOT, C. VINCENT, H. VINCENT, in "Matériaux Composites pour applications à hautes températures", edited by R. Naslain, J. Lamalle and J. L. Zullian (AMAC Paris, 1990) p. 55.
13. D. T. CLARK, in "Handbook of X-Ray and Ultraviolet Photoelectron Spectroscopy", edited by P. Briggs (Heyden, 1977).
14. C. D. WAGNER, W. M. RIGGS, L. E. DAVIS, J. F. MOULDER and G. E. MUILENBERG, "Handbook of X-ray Photoelectron Spectroscopy" (Perkin Elmer, Eden Prairie, 1979).
15. H. KOZLOWSKI, *Carbon* **24** (1986) 357.

Received 3 December 1990
and accepted 13 May 1991